Electronic Supplementary Material (ESI) for Nanoscale.

Supplementary Information

Co-doping optimized hydrogel-elastomer micro-actuator for versatile biomimetic motions

Yi Pan,[a] Lik Ho Lee,[a] Zhenyu Yang,[a] Sammer Ul Hassan[a] and Ho Cheung Shum[a,*]

[a.] Department of Mechanical Engineering, The University of Hong Kong, Pokfulam Road, Hong Kong, China

* E-mail: ashum@hku.hk

Experimental Section

Chemicals

The polydimethylsiloxane (PDMS) elastomer implemented in all cases was produced by Sylgard 184 silicone elastomer kit (DOWSIL, USA) mixed in a 10:1 base/cross-linker ratio. Graphene nanoplatelets (GNPs) and carbon nanotubes (CNTs) were purchased from TANFENG graphene Tech Co., Ltd. (China). Polyethylene glycol-modified gold nanoparticles (AuNPs), small diameter $Ti_3C_2T_x$ (MXene) thin layer dispersion solution, and carboxyl graphene dispersion solution were purchased from XFNANO materials Tech Co., Ltd. (China). N,N'-methylene-bis-acrylamide (BIS) was purchased from Sigma-Aldrich (Merck KGaA, Germany), while Fe_3O_4 nanoparticles (FeNPs), N-isopropylacrylamide (NIPAM) and benzophenone (BP) were purchased from Aladdin Industrial Corporation (China). Chloroform was purchased from Fisher Scientific. Deionized water was produced by a Milli-Q direct water purification system (Merck KGaA, Germany). All chemicals were used as received.

Fabrication of pNIPAM@GPDMS bilayer actuator

The experimental materials were prepared in the following ratios, except for the controlled experiments. The NIPAM solution was prepared by dissolving 9 wt% of NIPAM and 0.2 wt% of BIS in DI water. The BP solution was prepared by dissolving 40 wt% of BP in chloroform. BP and GNPs co-doped PDMS (G-PDMS) were prepared by mixing 7 wt% BP solution and 2 wt% GNPs into the PDMS prepolymer. The methodology for producing our hydrogel-elastomer bilayer actuator has been demonstrated in Fig. 2A. It was produced by firstly pouring the GPDMS precursor onto a glass slide. Then GPDMS was spin-coated at certain speeds ranging from 100 to 800 rpm for 1 min to obtain the desired thickness of the GPDMS layer (Fig. S5A). Next, the GPDMS film was placed on a hot plate at 85 °C for 15 min. Once the PDMS was fully cured, NIPAM solution was applied to the surface of the GPDMS. The pNIPAM grafting was performed in a UV chamber (ABM-USA, Inc., USA). The NIPAM was polymerized via irradiation with 365 nm UV light (12.8 mW/cm^2) for a specific time ranging from 5 to 30 min to get the desired thickness of the pNIPAM layer at ambient temperature (Fig. S5B). Once the pNIPAM was cross-linked, the bilayer was removed and washed with DI water.

In order to fabricate the pNIPAM@PDMS bilayer containing different kinds of dopants, we designed the dopants with similar dispersibility to the corresponding layers. Graphene, MXene, and AuNPs are water-dispersible, so they were mixed into the NIPAM solution, while GNPs, FeNPs, and CNTs are non-water-dispersible, so they were blended into PDMS.

Fabrication of soft robots

The spin coating speed used in fabricating the artificial flower, gripper and quadruped robot was 100 rpm. As shown in Fig. S7A, FeNPs-PDMS and GPDMS were dripped on a flat substrate before 15 min self-leveling to fabricate the caterpillar robot. For the spore robot, the applied spin-coating speed was 500 rpm, and after pNIPAM grafting, they were cut out by a laser cutter with 70% power and 15% speed (30W, VLS2.30DT, Universal Laser Systems, USA).

Microscopy

The pNIPAM@GPDMS bilayer was imaged by using a scanning electron microscope (Hitachi S3400N, Japan). Energy-dispersive x-ray scattering was used to obtain the elemental mapping of various elements in the cross-section of the bilayer. The graphene nanoplatelets were imaged by using a transmission electron microscope (Philips CM100, Netherlands). The fluorescence image of the pNIPAM layer in the bilayer structure was obtained using a fluorescence microscope (Leica Microsystem, Germany).

Responsiveness of the pNIPAM@GPDMS actuator

One end of the pNIPAM@GPDMS actuator (10 mm × 2 mm) was fixed to the edge of a horizontal platform and hanged horizontally. A humidifier was used to regulate the surrounding humidity to above 95% RH. The white light source (400 mW, LS-3000UV, QSPEC, China) was illuminated from a tilt angle of approximately 45 degrees. A digital camera was applied to record the bending and unbending performances of the actuators from the side view. In contrast, the thermal camera (ETS320, FLIR, USA) was placed directly above the actuators to monitor the photothermal phenomenon of the actuators.

Control of soft robots

The artificial flower, gripper, and quadruped robot were manipulated on an iced platform (ice placed under the glass slide) to maintain high relative humidity (~60%RH) and low temperature (~15 ℃) of their working environment. The optical fiber connection with the Xenon light source (400 mW, LS-3000UV, QSPEC, China) was applied above to manipulate the robots' movement. The caterpillar robot was manipulated on a glass slide coated with silicon dioxide microspheres to decrease the friction between the robot and the platform surface. Under the platform, a magnet (magnetic field intensity = 88 mT) was applied to anchor the robot. Above the platform, optical fiber and water drops were applied for the unbending and bending movements of the robot. In the dispersal and jumping experiments of spore robots, the experiments were performed on a glass

surface. A solar simulator (Halogen lamp, Philips, Netherlands) was used to attain a larger irradiation area.

The maximum weight lifting test of the gripper

A ball with a loop (diameter of the ball ≈ 5 mm; net weight = 0.170 g) was caught by the gripper in a high humidity environment (RH ≈ 100%) (**Fig. S8**). Then, a pan with a hook (net weight = 0.275 g) was carefully suspended on the loop. We kept adding weights (mass of each weight ≈ 0.024 g) into the pan until the ball fell out of the gripper. The maximum weight that the gripper can lift is the total mass of all objects before the last weight is put on the pan. The experiment was repeated five times.

High-speed imaging

To observe the jumping behavior of the spore robot during the light irradiation experiments, high-speed videos were obtained by using a high-speed camera (Fastcam SA4, Photron, USA). The camera was placed on the side of the robot, and the frame rate was set to 1000 fps. The camera software Photron Fastcam Viewer (PFV) was used to view the recorded movies, which were then processed using Tracker. (Open Source Physics, USA). The same observation method was applied in the spore robot's 'jumping over an obstacle' experiment, where the obstacle is a metallic ring with a height of 1.3 mm, an inner diameter of 6 mm, and an outer diameter of 8.6 mm.

Supplementary Notes

Note S1:

The equation for bending curvature (ρ) is deduced from Timoshenko theory on bi-material beam [1]:

$$\rho = \frac{1}{6\varepsilon}\left[3(\omega_1+\omega_2) + \frac{E_1\omega_1^3 + E_2\omega_2^3}{\omega_1+\omega_2}\left(\frac{1}{E_1\omega_1} + \frac{1}{E_2\omega_2}\right)\right]$$

where ε is the mismatch strain between the swelling and non-swelling layers. ω_1 and ω_2 denote the thickness of each layer, while E_1 and E_2 denote the Young's modulus of the corresponding layer.

Supplementary Figures

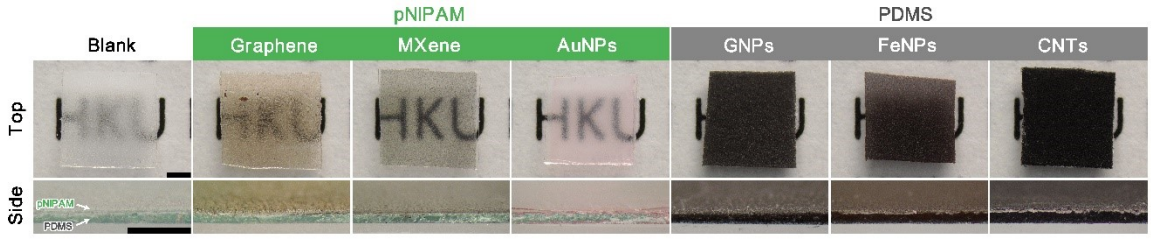

Fig. S1 Photographs of pNIPAM@PDMS with carboxyl graphene, small diameter $Ti_3C_2T_x$ (MXene) thin layer or gold nanoparticles (AuNPs) in pNIPAM layer, and graphene nanoplatelets (GNPs), Fe_3O_4 nanoparticles (FeNPs) or carbon nanotubes (CNTs) in PDMS layer. Scale bars: 1 mm.

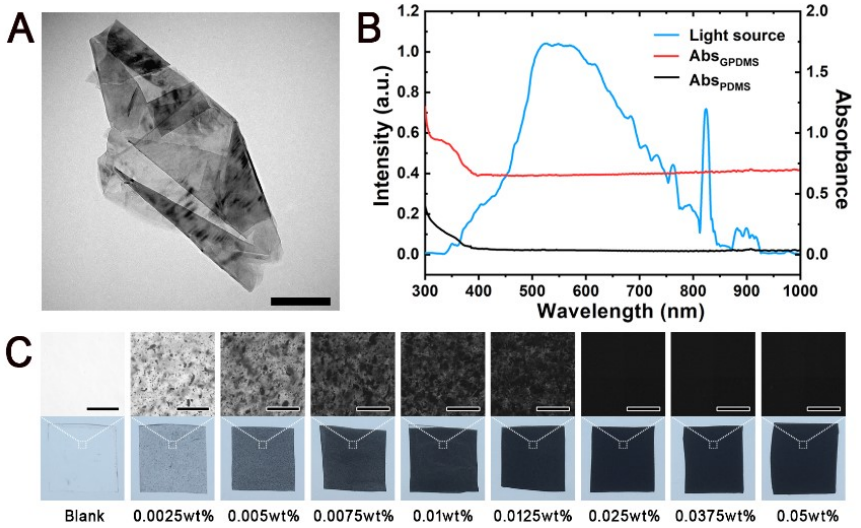

Fig. S2 (A) TEM imaging of GNPs. Scale bar: 400 nm. (B) The spectrum of the light source and absorption of GPDMS and PDMS, respectively. (C) Micrographs and photographs of GPDMS containing various amounts of GNPs. Scale bars: 500 μm.

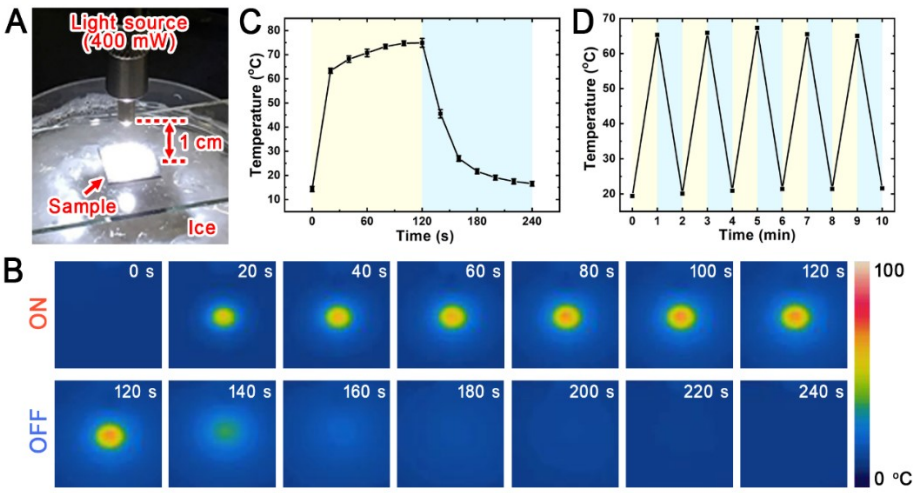

Fig. S3 (A) The set-up of photothermal testing. (B) Thermal images of GPDMS with and without ligth irradiation. (C) Dynamical process of thermal response of GPDMS. Yellow background: light

irradiation. Blue background: without light irradiation. (D) Repeatability test of the photothermal behavior of GPDMS.

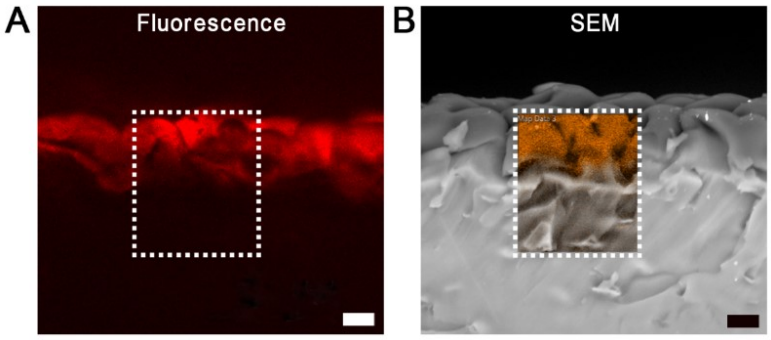

Fig. S4 Comparison of the fluorescence microscope image (A) and SEM image overlapping with EDX mapping of the carbon-rich region (B) at the cross section of the hydrogel-elastomer bilayer. Scale bars: 10 μm.

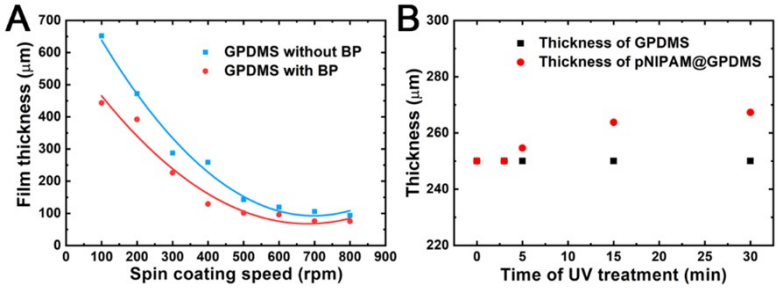

Fig. S5 (A) Spin coating dependent film thickness of the GPDMS. (B) Thickness of pNIPAM layer versus the time of UV treatment.

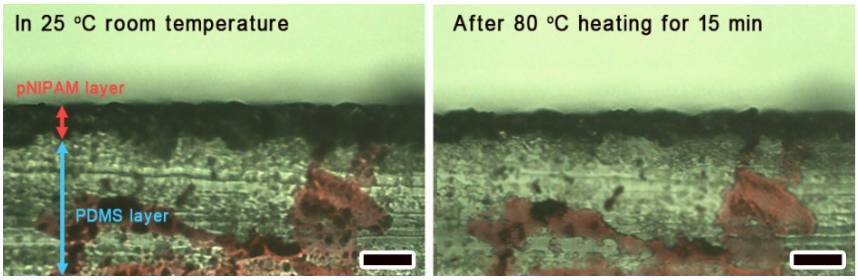

Fig. S6 Optical microscope images of the hydrogel-elastomer cross section (Left) at 25 °C room temperature and (Right) after 80 °C heating for 15 min. Scale bars: 20 μm.

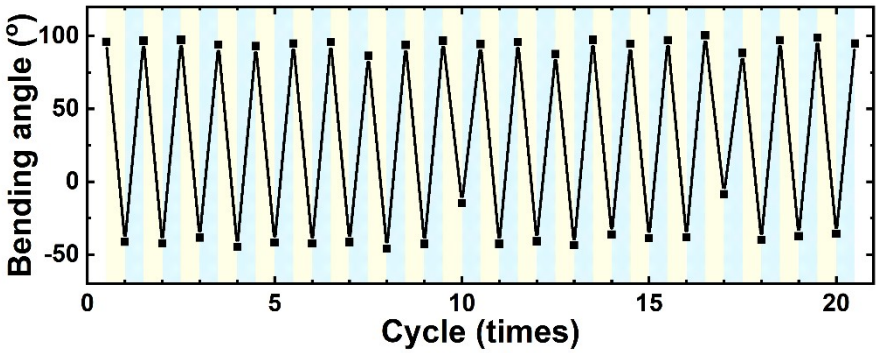

Fig. S7 Cyclic test of the pNIPAM@GPDMS actuator (thickness = 289 μm) between 1 min of humidification (blue background, RH ≈ 100%) and 1 min of light irradiation (yellow background, power = 400 mW).

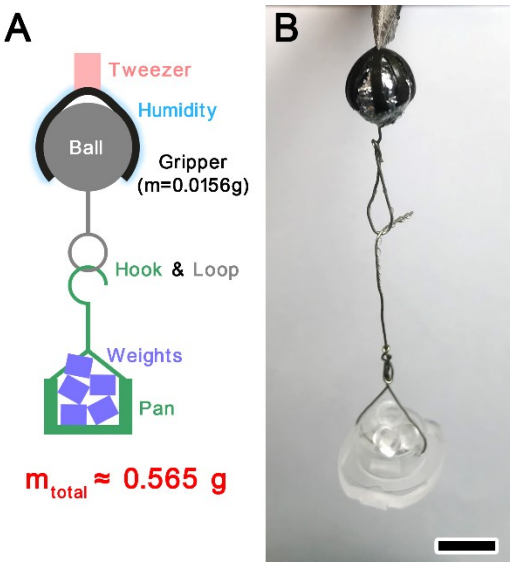

Fig. S8 (A) Schematic illustration and (B) photograph of the maximum lifting weight test of the gripper. Scale bar: 5 mm.

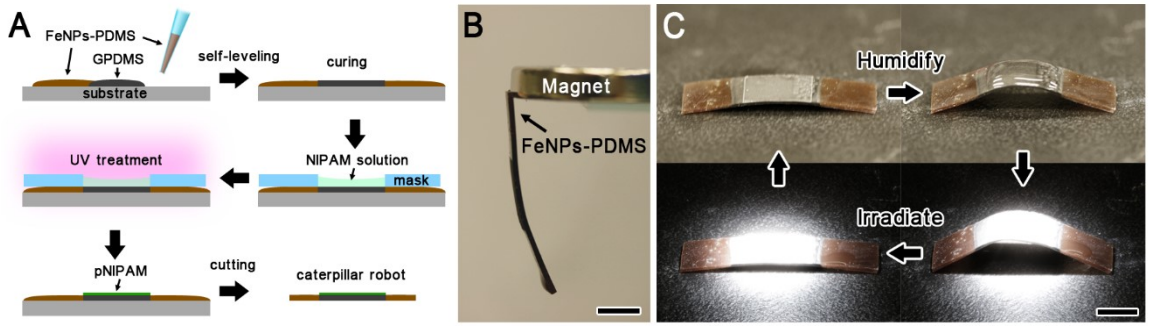

Fig. S9 (A) Schematic of the fabrication of caterpillar robot. (B) The magnetic end of caterpillar robot. Scale bar: 5 mm. (C) Humidity and light responsiveness of the caterpillar robot. Scale bar: 5 mm.

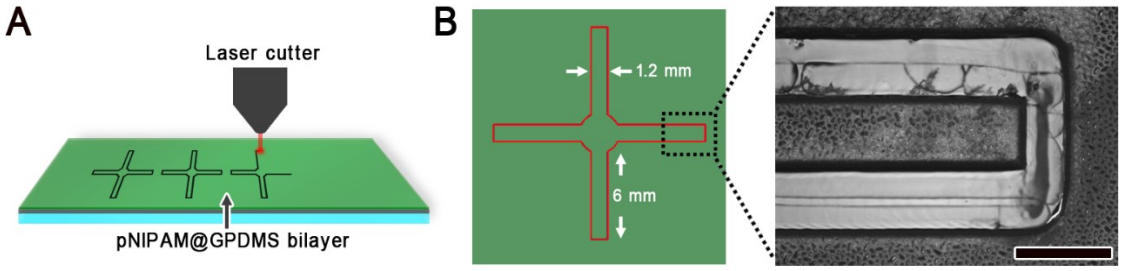

Fig. S10 (A) Fabrication of spore robot by laser cutting of pNIPAM@GPDMS bilayer. (B) The design blueprint of the spore robot and the actual cutting edge. Scale bar: 1 mm.

Supplementary Tables

Table S1. A comparison of thickness parameters of the responsive hydrogel-elastomer actuator samples in the current study

Thickness of hydrogel layer (μm)	Thickness of elastomer layer (μm)	Thickness ratio[a]	References
200	100	2	2
1000	1000	1	3
800	500	1.6	4
113	300	0.38	5
14	155	0.09	This work

[a.] Thickness ratio = Thickness of hydrogel layer/Thickness of elastomer layer

Supplementary Movies

Movie S1. Stimuli-responsiveness of pNIPAM@GPDMS actuator.

Movie S2. Comparison of pNIPAM@GPDMS and pNIPAM@PDMS in light responsiveness.

Movie S3. Nastic movement of artificial flower.

Movie S4. Catch and release of gripper.

Movie S5. Repeatability test of the gripper.

Movie S6. Crawling of quadruped robot.

Movie S7. Inching of caterpillar robot.

Movie S8. Dispersal of spore robots.

Movie S9. Jumping of a spore robot.

Movie S10. Spore robot jumps over an obstacle.

References

1. Y. Wu, X. Hao, R. Xiao, J. Lin, Z. L. Wu, J. Yin and J. Qian, *Acta Mech. Solida Sin.*, 2019, **32**, 652.
2. H. Li, Y. Liang, G. Gao, S. Wei, Y. Jian, X. Le, W. Lu, Q. Liu, J. Zhang and T. Chen, *Chem. Eng. J.*, 2021, **415**, 128988.
3. A. M. Hubbard, W. Cui, Y. Huang, R. Takahashi, M. D. Dickey, J. Genzer, D. R. King and J. P. Gong, *Matter*, 2019, **1**, 674.
4. X. Li, X. Cai, Y. Gao and M. J. Serpe, *J. Mater. Chem. B*, 2017, **5**, 2804.
5. H. Lin, S. Ma, B. Yu, X. Pei, M. Cai, Z. Zheng, F. Zhou and W. Liu, *Chem. Mater.*, 2019, **31**, 9504.